

UltraVSR: Achieving Ultra-Realistic Video Super-Resolution with Efficient One-Step Diffusion Space

Yong Liu
Xi'an Jiaotong University
Xi'an, China
liuy1996v@qq.com

Jinshan Pan
Nanjing University of Science and
Technology
Nanjing, China
sdluran@gmail.com

Yinchuan Li
Huawei Noah's Ark Lab
Beijing, China

Qingji Dong
Xi'an Jiaotong University
Xi'an, China

Chao Zhu
Xi'an Jiaotong University
Xi'an, China

Yu Guo
Xi'an Jiaotong University
Xi'an, China

Fei Wang*
Xi'an Jiaotong University
Xi'an, China
wfx@xjtu.edu.cn

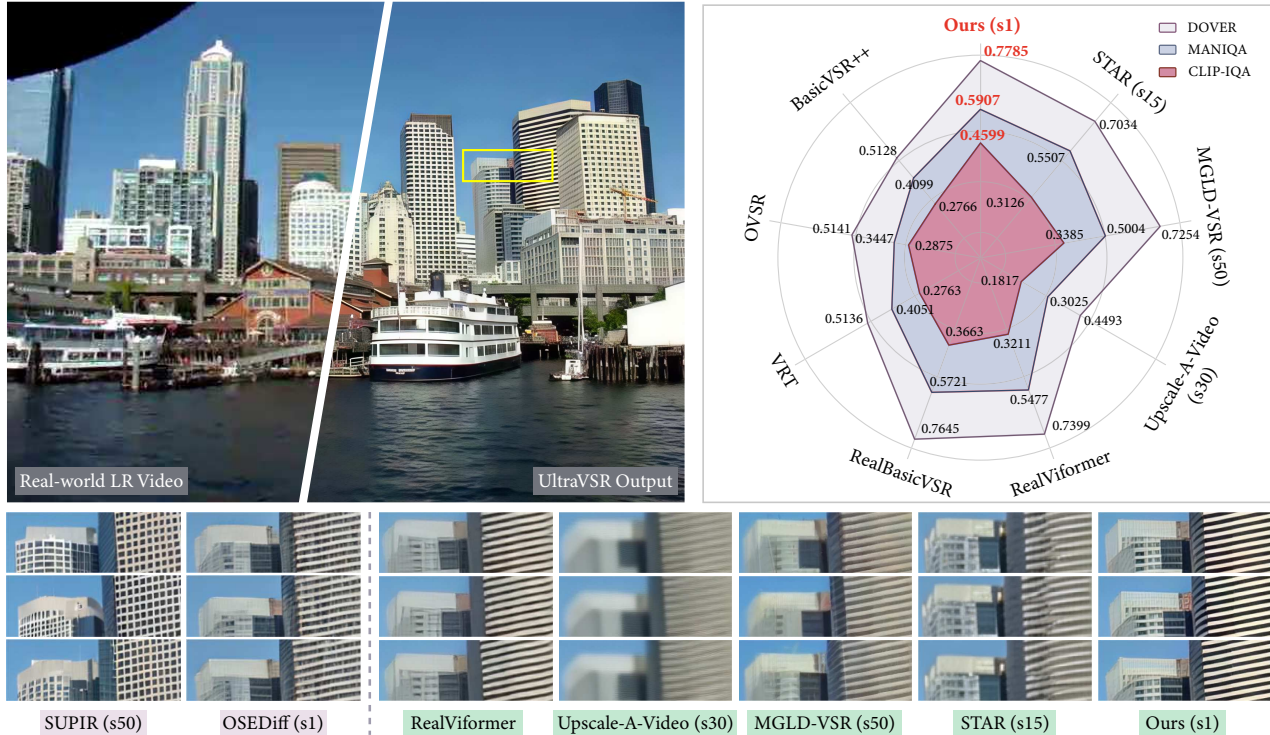


Figure 1: Quantitative and qualitative VSR comparisons. Top-left: An example on a real-world low-resolution (LR) video frame; Top-right: Quantitative comparison with state-of-the-art VSR approaches on the VideoLQ benchmark [8]; Bottom: Visual comparison against both SISR approaches and VSR approaches across three consecutive frames. Our one-step (s1) approach achieves leading scores across all three metrics with visually realistic and temporally coherent results.

*Corresponding author. Author affiliation: National Key Laboratory of Human-Machine Hybrid Augmented Intelligence, National Engineering Research Center of Visual Information and Applications, Institute of Artificial Intelligence and Robotics, Xi'an Jiaotong University.

Permission to make digital or hard copies of all or part of this work for personal or classroom use is granted without fee provided that copies are not made or distributed for profit or commercial advantage and that copies bear this notice and the full citation

on the first page. Copyrights for components of this work owned by others than the author(s) must be honored. Abstracting with credit is permitted. To copy otherwise, or to post on servers or to redistribute to lists, requires prior specific permission and/or a fee. Request permissions from permissions@acm.org.
MM '25, Dublin, Ireland.

© 2025 Copyright held by the owner/author(s). Publication rights licensed to ACM.
ACM ISBN 979-8-4007-2035-2/2025/10
<https://doi.org/10.1145/3746027.3755117>

Abstract

Diffusion models have shown great potential in generating realistic image detail. However, adapting these models to video super-resolution (VSR) remains challenging due to their inherent stochasticity and lack of temporal modeling. Previous methods have attempted to mitigate this issue by incorporating motion information and temporal layers. However, unreliable motion estimation from low-resolution videos and costly multiple sampling steps with deep temporal layers limit them to short sequences. In this paper, we propose UltraVSR, a novel framework that enables ultra-realistic and temporally-coherent VSR through an efficient one-step diffusion space. A central component of UltraVSR is the Degradation-aware Reconstruction Scheduling (DRS), which estimates a degradation factor from the low-resolution input and transforms the iterative denoising process into a single-step reconstruction from low-resolution to high-resolution videos. To ensure temporal consistency, we propose a lightweight Recurrent Temporal Shift (RTS) module, including an RTS-convolution unit and an RTS-attention unit. By partially shifting feature components along the temporal dimension, it enables effective propagation, fusion, and alignment across frames without explicit temporal layers. The RTS module is integrated into a pretrained text-to-image diffusion model and is further enhanced through Spatio-temporal Joint Distillation (SJD), which improves temporal coherence while preserving realistic details. Additionally, we introduce a Temporally Asynchronous Inference (TAI) strategy to capture long-range temporal dependencies under limited memory constraints. Extensive experiments show that UltraVSR achieves state-of-the-art performance, both qualitatively and quantitatively, in a single sampling step. Code is available at <https://github.com/yongliuy/UltraVSR>.

CCS Concepts

• **Computing methodologies** → **Reconstruction**; *Image processing*; Computational photography.

Keywords

Video super-resolution, Diffusion model, Temporal consistency

ACM Reference Format:

Yong Liu, Jinshan Pan, Yinchuan Li, Qingji Dong, Chao Zhu, Yu Guo, and Fei Wang. 2025. UltraVSR: Achieving Ultra-Realistic Video Super-Resolution with Efficient One-Step Diffusion Space. In *Proceedings of the 33rd ACM International Conference on Multimedia (MM '25)*, October 27–31, 2025, Dublin, Ireland. ACM, New York, NY, USA, 10 pages. <https://doi.org/10.1145/3746027.3755117>

1 Introduction

Video super-resolution (VSR) aims to reconstruct high-resolution (HR) videos from low-resolution (LR) inputs, a task that has garnered significant attention in multimedia and computer vision communities. Unlike single-image super-resolution (SISR), VSR presents additional challenges due to the necessity of maintaining temporal consistency across frames while recovering high-frequency details. With the rapid advancement of deep learning, numerous VSR approaches [1, 6, 7, 11, 14, 17, 23, 49] have emerged over the past decade. However, these methods still struggle to restore realistic textures under complex and unknown real-world degradations.

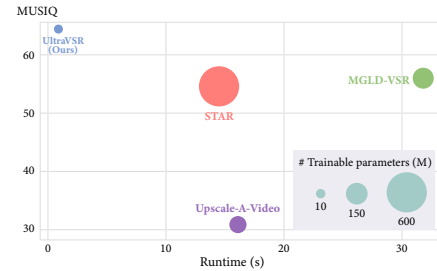


Figure 2: Comparison of runtime and metrics among diffusion-based VSR approaches. Note that the runtime is measured with the HR sequence upscaled to 720×1280. Our approach achieves the fastest speed with better quality.

Diffusion models [15, 36] have achieved remarkable success in image synthesis [9, 34], image editing [19, 53] and SISR [41, 45]. However, adapting these models to VSR remains challenging due to the lack of temporal modeling capabilities. Additionally, the inherent randomness of the diffusion process further exacerbates temporal artifacts such as flickering across frames, e.g., the results of SUPIR [60] and OSEDiff [48] in Fig. 1. Recent approaches, such as MGLD-VSR [55] and Upscale-A-Video [65], have attempted to improve temporal consistency by integrating 3D convolutions, temporal attention mechanisms, and motion propagation modules into image diffusion models. Alternatively, text-to-video diffusion models have also been explored for VSR [51]. Nevertheless, these approaches suffer from high computational costs due to the use of temporal layers and unreliable motion information estimated from LR videos. Moreover, these approaches require a large number of sampling steps for each frame, making inference inefficient and impractical, especially for memory-constrained processing of high-resolution and long-duration video sequences.

This paper proposes UltraVSR, an efficient one-step diffusion model for real-world VSR. In contrast to multi-step VSR approaches, UltraVSR introduces a Degradation-aware Reconstruction Scheduling (DRS) that reformulates the conventional multi-step iterative denoising paradigm as a single-step reconstruction process. DRS first estimates a degradation factor from the input LR video and then maps it with the diffusion noise schedule, thereby achieving single-step reconstruction from LR input to HR video. This scheme eliminates the randomness in the diffusion process and significantly improves computational efficiency. To maintain temporal consistency across frames, we develop a lightweight yet effective Recurrent Temporal Shift (RTS) module, which enables efficient inter-frame feature propagation, fusion, and alignment through two novel units: (1) RTS-convolution unit, which partitions feature maps by channels and shifts groups temporally across adjacent frames for localized feature alignment using 2D convolution; (2) RTS-attention unit, which incorporates temporal shifting operations on *Key/Value* tensors prior to self-attention computation, allowing the model to capture global contextual dependencies.

During training, the RTS module is embedded into a pretrained text-to-image diffusion model and subsequently optimized through Spatio-temporal Joint Distillation (SJD). SJD introduces dual temporal regularizers to separately model real and synthetic video distributions. By minimizing both spatial and temporal gradient discrepancies between two distributions, SJD effectively guides the

one-step reconstruction process toward producing visually realistic and temporally consistent HR videos. At inference, we further propose a memory-efficient Temporally Asynchronous Inference (TAI) strategy that decouples spatial and temporal processing by segmenting long video sequences into mini-batches, which are processed independently and then merged prior to RTS propagation. In this way, TAI significantly reduces memory overhead while enabling the model to capture long-range temporal dependencies. Experiments demonstrate that UltraVSR achieves better performance with significantly faster inference, as shown in Fig. 1 and Fig. 2.

In summary, the main contributions of this paper are as follows:

- We propose UltraVSR, an efficient one-step diffusion framework by introducing a Degradation-aware Reconstruction Scheduling (DRS) for high-quality video reconstruction. To the best of our knowledge, this is the first work to tackle the VSR problem in just one sampling step.
- We develop a lightweight Recurrent Temporal Shift (RTS) that enables effective feature propagation, fusion, and alignment across frames by partially shifting feature components temporally, without relying on explicit temporal layers.
- We introduce Spatio-temporal Joint Distillation (SJD) to enhance temporally coherence and content realism, and propose Temporally Asynchronous Inference (TAI) for memory-efficient long-range dependency modeling.
- Extensive experiments show that UltraVSR outperforms state-of-the-art methods in both visual quality and temporal consistency, while significantly accelerating inference speed.

2 Related Work

2.1 Real-World VSR

Numerous VSR methods [6, 11, 14, 23, 24, 27, 50] have been developed to enhance video quality under real-world degradation. For instance, Chan *et al.* proposed RealBasicVSR [8], which removes degradations in videos by introducing a pre-cleaning module and a stochastic degradation scheme. More recently, Zhang *et al.* introduced a channel-attention-based recurrent model, RealVformer [63], based on findings from investigating channel and spatial attention in a real-world setting. Despite these advancements, many approaches remain sensitive to complex degradations due to limited modeling capacity, leading to poor generalization.

2.2 Diffusion Model-based VSR

Diffusion models [15, 36] have demonstrated strong performance in generating realistic details [3, 19, 25, 34, 53, 56]. Recent studies have attempted to scale up diffusion models for the VSR task in two ways. On one hand, Zhou *et al.*[65] and Yang *et al.*[55] leverage image diffusion models and propose Upscale-A-Video and MGLD-VSR, respectively, by incorporating additional temporal layers and motion information. On the other hand, Xie *et al.*[51] build upon a pretrained text-to-video diffusion model and introduce STAR, which employs ControlNet[62] to inject LR video information into the generation process. However, these approaches often rely on multiple sampling steps and complex temporal layers, resulting in high inference latency. To overcome these challenges, we propose an efficient one-step diffusion model for real-world VSR.

3 Proposed Method

3.1 Overview

Our UltraVSR is built upon the pretrained Stable Diffusion model [34], comprising a VAE encoder/decoder, a text encoder, and a diffusion UNet, as illustrated in Fig.3. To construct an efficient one-step reconstruction model G_θ to generate HR video V_{HR} from LR input V_{LR} , we introduce three key components: (i) Degradation-aware Reconstruction Scheduling (DRS): Defines a one-step reconstruction from LR videos to HR videos (Sec. 3.2); (ii) Recurrent Temporal Shift (RTS) Module: Incorporates temporal dependencies into the diffusion model by shifting specific feature components across frames, without relying on explicit temporal layers (Sec. 3.3); (iii) Spatio-temporal Joint Distillation (SJD): Guides training with the content realistic and temporal coherent supervision (Sec. 3.4).

Given an input LR video sequence V_{LR} , UltraVSR first estimates a degradation factor d and determines a corresponding reconstruction time step t_{rec} . Concurrently, a text prompt is simultaneously extracted from V_{LR} via the text encoder, while a latent representation z_{LR} is derived using the VAE encoder. These variables are fed into the diffusion UNet together to produce intermediate estimates $est.$, which are subsequently refined through DRS to obtain the HR latent representation z_{HR} . Finally, z_{HR} is passed to the VAE decoder to produce the high-quality HR output V_{HR} .

During training, we incorporate LoRA layers [16] into both the VAE encoder and diffusion UNet, achieving efficient parameter tuning while preserving generation priors. To ensure temporal consistency throughout the reconstruction process from V_{LR} to V_{HR} , we integrate the RTS module across multiple scales of both the diffusion UNet and VAE decoder, components identified as primary sources of temporal flickering artifacts in the original architecture [55, 65]. SJD is further used to enforce that the one-step reconstruction model generates V_{HR} with both spatial realism and temporally coherence. The detailed network architectures are provided in the supplementary materials. We also propose a Temporally Asynchronous Inference (TAI) strategy for memory-efficient long-range dependency modeling in Sec. 3.5.

3.2 Degradation-aware Reconstruction Scheduling

Standard diffusion models (DDPMs) [15, 36] assume a forward diffusion process that gradually adds noise to real data z_0 following a fixed noise schedule:

$$z_t = \sqrt{\bar{\alpha}_t} z_0 + \sqrt{1 - \bar{\alpha}_t} \epsilon. \quad (1)$$

where $t \in \{0, 1, 2, \dots, T\}$, $\bar{\alpha}_t = \prod_{i=0}^t \alpha_i$ is a hyperparameter controlling the noise strength. The reverse diffusion process iteratively denoises from z_T to z_0 , but this inherently results in computationally expensive inference.

Inspired by the consistency models [37] and one-step generation models [31, 42, 59] that map the point z_t on the diffusion trajectory to the starting point z_0 directly, we introduce DRS to enable a one-step reconstruction from LR latent z_{LR} to HR latent z_{HR} .

As shown in Fig. 3 (a), we first estimate a degradation factor $d \in [0, 1]$ to quantify the degradation severity of V_{LR} :

$$d = DEM(V_{LR}), \quad (2)$$

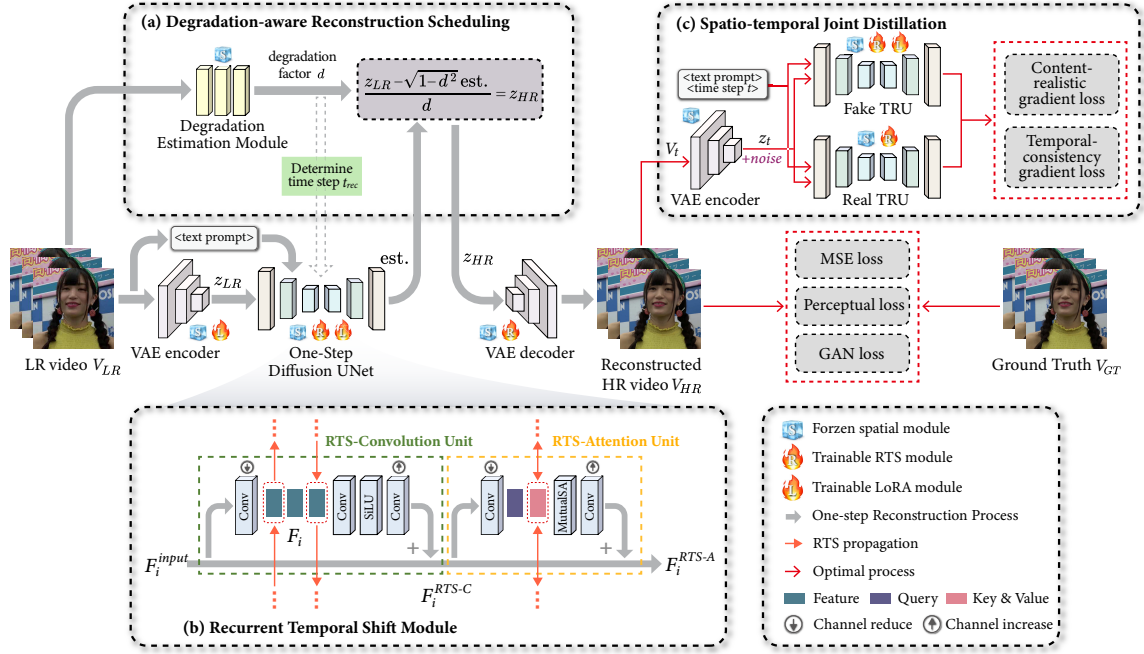


Figure 3: Training framework of the proposed UltraVSR.

where the degradation estimation module (DEM) is implemented using the pretrained CLIP model [41], which is a widely used no-reference quality assessment model. Here, $d = 0$ corresponds to maximal video degradation, while $d = 1$ indicates minimal degradation. This is consistent with the diffusion process described in Eq. 1: a lower $\bar{\alpha}_t$ pushes z_t closer to Gaussian noise, whereas a higher $\bar{\alpha}_t$ retains stronger fidelity to the real data distribution. Therefore, we formulate a direct mapping between the degradation factor d and the noise schedule by defining $d = \sqrt{\bar{\alpha}_t}$, mathematically linking perceptual quality to the denoising process. In this way, the HR latent representation z_{HR} can be derived as:

$$z_{HR} = \frac{z_{LR} - \sqrt{1 - d^2} \text{est.}}{d}, \quad (3)$$

where est. denotes the diffusion UNet's output.

Additionally, we determine the reconstruction time step t_{rec} through nearest-neighbor matching against the predefined noise schedule $\{\sqrt{\bar{\alpha}_t}\}_{t=1}^T$:

$$t_{rec} = \arg \min_t |d - \sqrt{\bar{\alpha}_t}|, \quad (4)$$

selecting the time step where $\sqrt{\bar{\alpha}_{t_{rec}}}$ most closely approximates the degradation factor d . This mechanism enables efficient one-step reconstruction by leveraging the pretrained generative prior.

3.3 Recurrent Temporal Shift Module

The key to VSR lies in effectively aggregating complementary spatio-temporal information from misaligned frames. To this end, we propose a lightweight yet effective Recurrent Temporal Shift (RTS) module that captures spatio-temporal dependencies without relying on computationally expensive temporal layers. As illustrated in Fig.3 (b), the RTS module performs temporal feature propagation by bidirectionally shifting partitioned features across

adjacent frames in a parameter-free manner, inspired by [5, 28, 29]. It consists of two core components: the RTS-Convolution Unit and the RTS-Attention Unit, which collaborate to enable efficient information exchange across neighboring frames. To improve computational efficiency, we apply channel-reducing and channel-increasing convolutions at the beginning and end of each unit, respectively.

3.3.1 RTS-Convolution Unit. Given an intermediate feature map $F_i = \text{Conv}(F_i^{\text{input}}) \in \mathbb{R}^{C \times h \times w}$ for the i -th frame, RTS divides it into three equal channel-wise segments: F_i^{-1} , F_i^0 , and F_i^1 , where each segment $F_i^j \in \mathbb{R}^{T \times \frac{C}{3} \times h \times w}$. These segments are then shifted along the temporal dimension with offsets of +1, 0, and -1, respectively, where a positive offset denotes a forward shift, a negative offset denotes a backward shift, and zero implies no shift. The aggregated features for the i -th frame are then obtained by concatenating the temporally shifted feature segments:

$$F_i^{\text{Agg}} = \text{Concat}(F_{i-1}^{-1}, F_i^0, F_{i+1}^1). \quad (5)$$

This strategy ensures that each frame receives contextual information from both past and future frames. To maintain consistent dimensions throughout the video, zero-padding is applied at the sequence boundaries. The aggregated features are processed via convolutional layers with ReLU activation followed by a residual connection to perform local temporal alignment:

$$F_i^{\text{RTS-C}} = \text{Conv}(\text{ReLU}(\text{Conv}(F_i^{\text{Agg}}))) + F_i^{\text{input}}. \quad (6)$$

3.3.2 RTS-Attention Unit. Building on the observation that attention-based feature alignment inherently captures strong semantic priors in diffusion models [2, 5, 12, 38], we further develop an RTS-attention unit to aggregate high-level global contextual dependencies across frames. Given the *Query*, *Key*, and *Value* embeddings $\{Q_i, K_i, V_i\} = \text{Conv}(F_i^{\text{RTS-C}})$ for the i -th frame, RTS shifts K_i and V_i

forward and backward temporally, allowing the model to query semantically correlated structures and textures from adjacent frames. We adopt Mutual Self-Attention (MutualSA) [5] to aggregate semantic information across frames:

$$F_i^{MSA} = \sum_{j=-1}^1 \text{MutualSA}(Q_i, K_{i+j}, V_{i+j}), \quad (7)$$

where $\text{MutualSA}(Q_i, K_{i+j}, V_{i+j}) = \text{Softmax}(\frac{Q_i K_{i+j}^T}{\sqrt{r}}) V_{i+j}$, r denotes the embedding dimension. The final output of the RTS-Attention Unit is obtained by:

$$F_i^{RTS-A} = \text{Conv}(F_i^{MSA}) + F_i^{RTS-C}. \quad (8)$$

Unlike conventional spatial self-attention, which operates independently on each frame, the RTS-attention unit aligns semantic information across the temporal dimension, thereby enhancing the temporal consistency of the reconstructed video.

3.4 Spatio-temporal Joint Distillation

To guide the proposed one-step reconstruction in generating visually realistic and temporally consistent HR videos, we introduce a dual-constrained optimization strategy, termed Spatio-temporal Joint Distillation (SJD). Our SJD shares motivation with other distribution matching generative models, such as SDS [33] and VSD [46, 59], but extends these paradigms from the image domain to video, explicitly modeling inter-frame temporal consistency dependencies.

As illustrated in Fig.3 (c), SJD introduces two Temporal Regularized UNets (TRU), a real TRU $\mathcal{T}_{\text{real}}$ and a fake TRU $\mathcal{T}_{\text{fake}}$. They are derived by integrating our proposed RTS module into the Stable Diffusion model [34]. During the training of the one-step reconstruction model G_θ , $\mathcal{T}_{\text{real}}$ and $\mathcal{T}_{\text{fake}}$ are dynamically updated using ground-truth video V_{GT} and the synthesized output V_{HR} , respectively. To capture both spatial realism and temporal consistency, we convert the noise predictions into video distributions using Eq. 1 at the output of the TRUs. Conceptually, $\mathcal{T}_{\text{real}}$ can be interpreted as providing gradient directions that encourage the reconstruction to become more realistic and temporally coherent. In contrast, $\mathcal{T}_{\text{fake}}$ yields gradients that reflect undesirable characteristics such as visual artifacts and temporal flickering. To this end, we formulate the gradient update rule for G_θ by integrating a content-realistic gradient loss and a temporal-consistency gradient loss:

$$\nabla \mathcal{L}_{\text{SJD}} = \nabla \mathcal{L}_{\text{realistic}} + \lambda \nabla \mathcal{L}_{\text{consistency}}, \quad (9)$$

where λ balances content realism and temporal coherence of V_{HR} . This encourages the synthesized V_{HR} toward higher perceptual realism and temporal coherence while suppressing visual artifacts and flickering. The content-realistic gradient loss is formulated as:

$$\nabla \mathcal{L}_{\text{realistic}} = \mathbb{E} \left[\omega(t) (\mathcal{T}_{\text{real}}(z_t, t) - \mathcal{T}_{\text{fake}}(z_t, t)) \frac{dG}{d\theta} \right], \quad (10)$$

where $z_t = \sqrt{\bar{\alpha}_t} z_0 + \sqrt{1 - \bar{\alpha}_t} \epsilon$, $z_0 = \mathcal{E}(V_{HR})$, $V_{HR} = G_\theta(V_{LR})$, $\epsilon \sim \mathcal{N}(0, \mathbf{I})$, \mathcal{E} denotes the pretrained VAE encoder, $\omega(t)$ is a weighting coefficient to normalize the gradient magnitudes across varying noise levels [59]. The temporal-consistency gradient loss enhances temporally coherence by penalizing discrepancies in the inter-frame

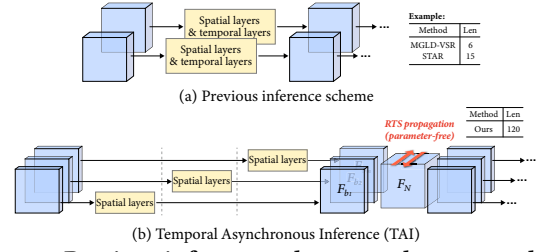


Figure 4: Previous inference scheme vs. the proposed TAI.

gradients of two TRUs:

$$\begin{aligned} \nabla \mathcal{L}_{\text{consistency}} = & \mathbb{E} \left[\omega(t) \left((\mathcal{T}_{\text{real}}(z_t, t)[:-1] - \mathcal{T}_{\text{real}}(z_t, t)[1:]) \right. \right. \\ & \left. \left. - (\mathcal{T}_{\text{fake}}(z_t, t)[:-1] - \mathcal{T}_{\text{fake}}(z_t, t)[1:]) \right) \frac{dG}{d\theta} \right]. \end{aligned} \quad (11)$$

3.5 Temporally Asynchronous Inference

Existing diffusion-based VSR methods exhibit critical dependencies on temporal modules, incurring prohibitive memory overheads. As a result, such models require video segmentation into short clips for piecewise processing, as shown in Fig. 4 (a). For instance, under 48GB GPU memory constraints (NVIDIA RTX 8000), MGLD-VSR [55] processes ≤ 6 frames while STAR [51] handles ≤ 15 frames for 2K (1440 \times 2560) reconstruction. This fragmentation disrupts temporal continuity and fundamentally limits long-range dependency modeling. UltraVSR circumvents this limitation through implicit temporal modeling via RTS propagation, eliminating explicit temporal layers. Building on this architectural innovation, we propose a Temporally Asynchronous Inference (TAI) strategy that enables efficient capture of long-range temporal dependencies.

As illustrated in Fig. 4 (b), given an N -frames low-resolution video V_{LR} , TAI first divides it into m non-overlapping sub-sequences $\{V_{LR_1}, V_{LR_2}, \dots, V_{LR_m}\}$, each containing b frames. Then, these sub-sequences are processed sequentially through 2D spatial layers to obtain feature maps $\{F_{b_1}, F_{b_2}, \dots, F_{b_m}\}$, drastically reducing peak memory consumption. At the beginning of the RTS propagation, all these features are concatenated into a unified feature tensor F_N , which is then augmented by bidirectional RTS propagation to achieve efficient temporal information exchange between frames. The temporally shifted features are then divided back into sub-sequences for further refinement.

As a result, TAI enables memory-efficient inference while maintaining long-term temporal dependencies, capable of processing up to 120 frames at 1440 \times 2560 resolution identical hardware constraints, an $8\times$ throughput improvement over STAR [51]. This breakthrough makes UltraVSR particularly suitable for high-quality reconstruction of long-duration video sequences under resource-limited environments.

4 Experiments

4.1 Experimental Settings

4.1.1 Datasets. Similar to the most VSR approaches [8, 55, 63], we combine the training and validation sets from the REDS dataset [30] for model training, reserving four sequences (REDS4) for testing. We evaluate UltraVSR on four synthetic datasets (i.e., REDS4,

Table 1: Quantitative comparison with state-of-the-art VSR approaches on both synthetic and real-world benchmarks. The best and second best results are **highlighted and underlined, respectively.**

Datasets	Metrics	BasicVSR++ [7]	OVSr [57]	RealBasicVSR [8]	VRT [26]	RealViFormer [63]	Upscale-A-Video [65]	MGLD-VSR [35]	STAR [51]	Ours
REDS4	PSNR	33.77	23.55	28.59	32.97	28.18	25.62	27.49	24.08	24.50
	SSIM	0.9173	0.6743	0.8066	0.9007	0.7896	0.6761	0.7783	0.6721	0.6962
	MUSIQ	67.00	54.44	<u>67.03</u>	65.68	64.58	32.30	58.94	60.94	70.07
	CLIP-IQA	0.3149	0.3383	0.3724	<u>0.3743</u>	0.3558	0.1843	0.2908	0.3047	0.4397
	MANIQA	<u>0.6752</u>	0.5887	0.6671	0.6699	0.6545	0.3138	0.5837	0.6123	0.6821
	DOVER	0.7182	<u>0.6620</u>	0.7209	0.7067	0.7152	0.4053	0.6717	<u>0.7227</u>	0.7304
SPMCS	PSNR	23.39	29.87	22.87	23.43	23.45	<u>24.10</u>	23.43	22.95	23.08
	SSIM	0.6516	0.8702	0.6087	<u>0.6543</u>	0.6153	0.6386	0.6372	0.6001	0.6202
	MUSIQ	62.57	57.10	<u>69.44</u>	63.44	66.10	56.31	64.08	55.14	69.92
	CLIP-IQA	0.4341	0.4597	<u>0.4838</u>	0.4388	0.4432	0.3353	0.4685	0.3888	0.5377
	MANIQA	0.6263	0.6057	<u>0.6282</u>	0.6134	0.6148	0.4798	0.5562	0.5640	0.6386
	DOVER	0.6711	0.6031	<u>0.7506</u>	0.6404	0.7206	0.5675	0.6431	0.6404	0.7616
UDM10	PSNR	<u>34.68</u>	27.12	31.31	36.03	31.84	29.48	29.50	27.93	27.96
	SSIM	<u>0.9406</u>	0.8318	0.8936	0.9501	0.9074	0.8458	0.8744	0.8284	0.8346
	MUSIQ	63.26	57.94	<u>66.01</u>	61.38	61.86	39.48	64.54	57.34	66.46
	CLIP-IQA	0.5091	0.4338	0.4903	0.4697	0.4356	0.2356	<u>0.5083</u>	0.3843	0.4818
	MANIQA	0.5729	0.5593	<u>0.6083</u>	0.5501	0.5699	0.3329	0.5495	0.5219	0.6167
	DOVER	0.7947	0.7789	<u>0.8248</u>	0.7709	0.8185	0.5500	0.7851	0.8061	0.8361
YouHQ40	PSNR	23.99	22.67	<u>25.26</u>	25.01	25.73	25.20	24.97	23.76	24.75
	SSIM	0.5999	0.5670	0.6857	0.6510	<u>0.6974</u>	0.6865	0.6984	0.6593	0.6954
	MUSIQ	49.43	45.54	62.12	41.45	<u>62.27</u>	35.86	56.42	41.47	62.71
	CLIP-IQA	0.3798	0.3442	<u>0.4661</u>	0.3879	0.4520	0.2460	0.3960	0.3435	0.4928
	MANIQA	0.5145	0.4710	<u>0.5539</u>	0.4622	0.5500	0.3401	0.4717	0.4198	0.5847
	DOVER	0.6914	0.6877	<u>0.8855</u>	0.6347	0.8657	0.6216	0.8116	0.8084	0.8872
VideoLQ	MUSIQ	37.32	29.89	<u>62.48</u>	37.94	58.66	30.88	55.99	54.59	64.42
	CLIP-IQA	0.2766	0.2875	<u>0.3663</u>	0.2763	0.3211	0.1817	0.3385	0.3126	0.4599
	MANIQA	0.4099	0.3447	<u>0.5721</u>	0.4051	0.5477	0.3025	0.5004	0.5507	0.5907
	DOVER	0.5128	0.5141	<u>0.7645</u>	0.5136	0.7399	0.4493	0.7254	0.7034	0.7785

**Figure 5: Visual comparisons on synthetic low-quality videos from SPMCS [58] and YouHQ40 [65] datasets.**

SPMCS [58], UDM10 [39], and YouHQ40 [65]) and a real-world dataset (i.e., VideoLQ [8]) that contains 50 real-world video sequences with diverse degradations. For both synthetic training and testing datasets, LR-HR video pairs are generated following the degradation pipeline of RealBasicVSR [8].

4.1.2 Training Details. We implement UltraVSR using the PyTorch framework and the Diffusers [32] library. The input sequence length is set to 6, with the spatial size cropped to 512×512 resolution. We freeze the original spatial modules of the pretrained Stable Diffusion model while only training the newly introduced LoRA and RTS modules. Adam [21] optimizer is employed as the optimizer with $\beta_1 = 0.9$ and $\beta_2 = 0.99$. We use a combination of MSE loss, perceptual loss, temporal GAN loss [64], and SJD regularization loss to train UltraVSR. The real and fake TRUs are trained by minimizing a standard denoising objective [15, 40]. The weighting coefficient λ is set to 0.5. The learning rate is set to 5×10^{-5} for all models.

4.1.3 Evaluation Metrics. We evaluate super-resolved video quality using three image-based quality metrics: MUSIQ [20], CLIP-IQA [41], and MANIQA [54], along with one video-specific quality

metric, DOVER [47]. DOVER assesses both content quality and temporal consistency from both aesthetic and technical perspectives. In addition, the full-reference metrics (i.e., PSNR and SSIM) are also given as a reference. However, it should be noted that they poorly respond to realistic visuals [4, 13, 18, 22, 60] and can not reliably evaluate the performance of diffusion-based VSR models.

4.2 Evaluation with State-of-the-art Methods

To validate the efficacy of UltraVSR, we conduct both quantitative and qualitative comparisons with state-of-the-art VSR methods: BasicVSR++ [7], OVSr [57], RealBasicVSR [8], VRT [26], RealViFormer [63], Upscale-A-Video [65], MGLD-VSR [35], and STAR [51]. Due to the extremely high memory requirements of STAR, we had to limit its output resolution to a maximum of 1440 pixels. In addition, we include comparisons with state-of-the-art SISR approaches (i.e., RealESRGAN [44], StableSR [43], SUPIR [60], ResShift [61] and OSediff [48]) in the supplementary materials.

4.2.1 Quantitative Comparison. As demonstrated in Tab. 1, we present the quantitative results with existing state-of-the-art VSR

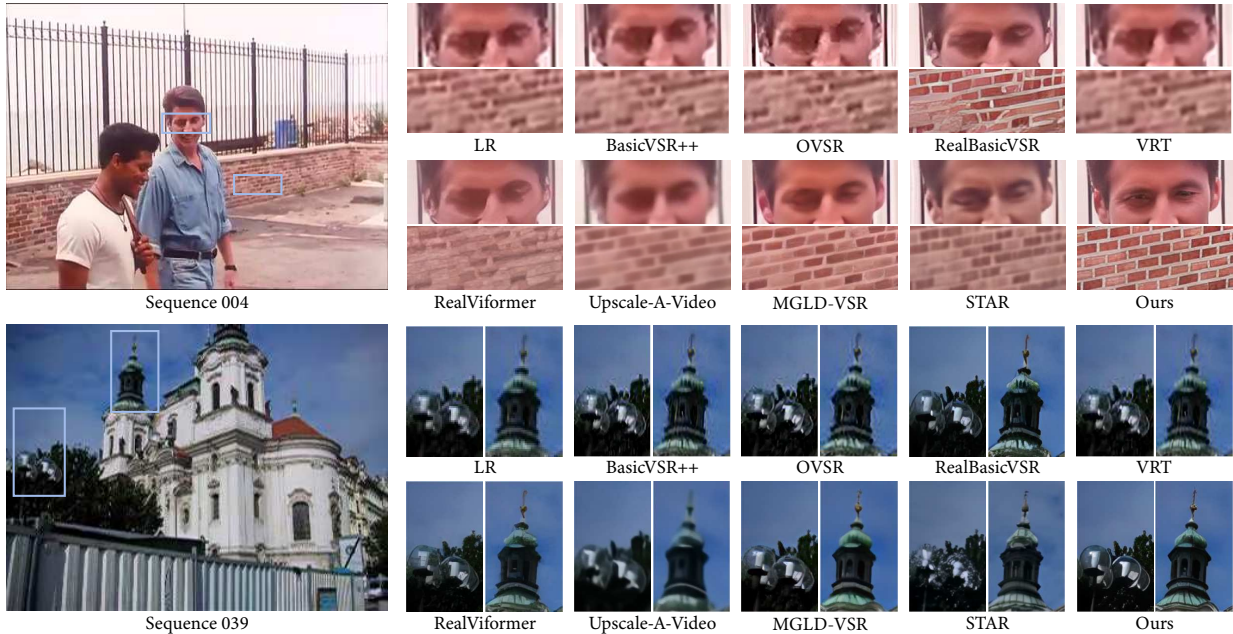


Figure 6: Visual comparisons on real-world low-quality videos from VideoLQ [8] dataset.

Table 2: Efficiency evaluations among diffusion-based VSR approaches. Both trainable/total parameters are measured for each model. The best results are highlighted.

Methods	Sampling step	Runtime (s)		# Params (M)
		720×1280	1440×2560	
Upscale-A-Video [65]	30	16.1	32.0	~ 96.6/746
MGLD-VSR [35]	50	31.8	204	156.0/1465
STAR [51]	15	14.5	110.2	629.9/2139
Ours	1	0.89	2.67	10.5/1912

approaches. It can be seen that our UltraVSR consistently achieves the highest score across nearly all non-reference metrics on all synthetic benchmarks, demonstrating its superior performance. Although approaches like BasicVSR++ [7] and VRT [26] have better performance in terms of PSNR or SSIM, they usually produce unsatisfactory results on real-world degraded videos (see Sec. 4.2.2), as reflected in their lower no-reference metric scores. As for the real-world VSR dataset VideoLQ [8], UltraVSR outperforms other methods across all non-reference metrics (MUSIQ: **+1.94**, CLIP-IQA: **+0.0936**, MANIQA: **+0.0186**, DOVER: **+0.014**). These notable improvements highlight UltraVSR’s strong ability to enhance complex and diverse real-world videos while preserving realistic details.

4.2.2 Qualitative Comparison. To further assess the effectiveness of the proposed UltraVSR, we present qualitative comparisons on both synthetic datasets (SPMCS [58] and YouHQ40 [65] in Fig. 5) and real-world dataset (VideoLQ [8] in Fig. 6). On synthetic videos, it can be observed that the competing approaches struggle to reconstruct accurate texture (e.g., the results of Upscale-A-Video [65] and STAR [51] in the first row) and blurriness (e.g., the results of RealViforformer [63] and the result of Upscale-A-Video [65] in the second row). In addition, MGLD-VSR [35] introduces color artifacts in the reconstructed frames. In contrast, our UltraVSR excels in restoring lost textures and structures under complex degradation scenarios,

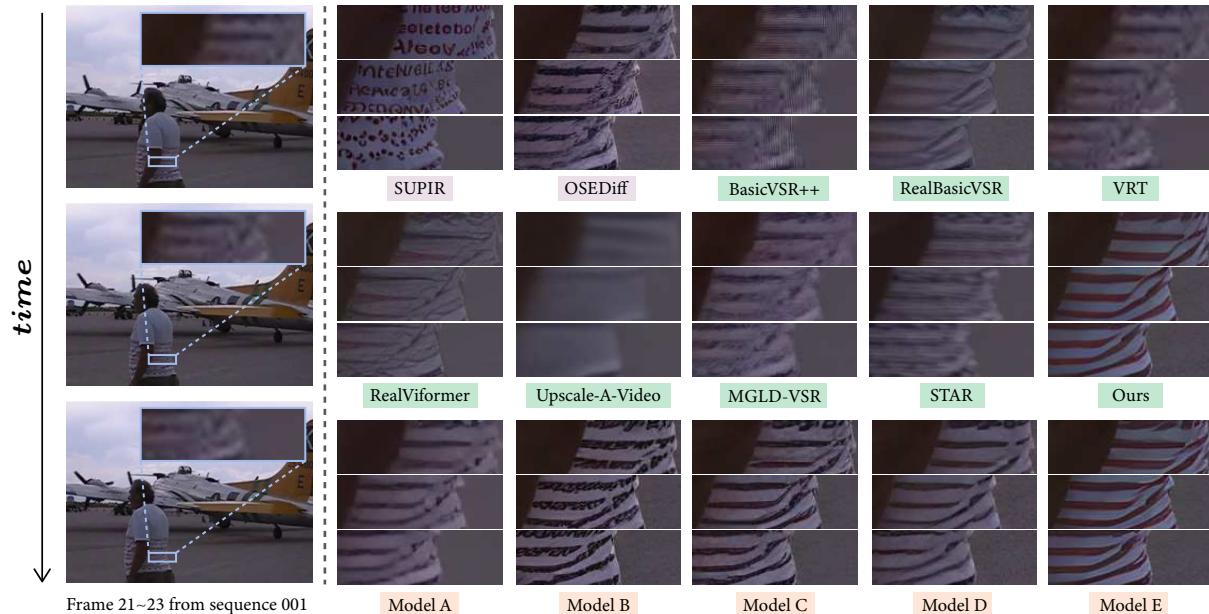
such as the outlines of statues and animal fur. On real-world videos, UltraVSR demonstrates superior texture reconstruction capabilities compared to competing approaches. For instance, in sequence 004, it not only recovers clear and realistic facial expressions but also faithfully reconstructs the structural details of the surrounding brick wall. In sequence 039, UltraVSR successfully restores intricate architectural details and decorations, demonstrating its robustness and generalization ability under challenging degradation scenarios. More comparisons can be found in the supplementary materials.

4.2.3 Temporal Consistency. From a quantitative perspective, we compare the DOVER metric, an effective video quality assessment approach, against competing methods in Tab. 1. Due to the inherent randomness in the diffusion model, the DOVER scores of existing diffusion-based VSR methods are generally low. Benefiting from the proposed one-step diffusion space, our UltraVSR achieves the best score on all the datasets (e.g., **+0.011** on the SPMCS dataset and **+0.014** on the VideoLQ dataset). In addition, Fig. 7 presents visual comparisons against both SISR and VSR approaches. It can be found that due to the inherent randomness and insufficient temporal modeling, results from SUPIR [60] and OSEDiff [48] exhibit severe temporal inconsistencies. While existing VSR approaches alleviate this issue, they often sacrifice texture details. In contrast, our ultraVSR successfully reconstructs videos with both fine texture structure and temporal coherence.

4.2.4 Efficiency Evaluations. To evaluate the efficiency of UltraVSR, we compare its sampling step, runtime, and parameters against other diffusion-based VSR approaches in Tab. 2. we assess computational efficiency at two common resolutions: 720p (720×1280) and 2K (1440×2560). All models were evaluated on a single NVIDIA RTX 8000 GPU. Existing diffusion-based VSR approaches typically require dozens of iterative sampling steps, resulting in prohibitively

Table 3: Ablation study of different configurations. Both trainable/total parameters of the one-step reconstruction model are measured for each model variant. The best and second best results are highlighted and underlined, respectively.

Models	DRS	RTS-Convolution Unit	RTS-Attention Unit	VSD [46, 59]	SJD	TAI	MUSIQ	CLIP-IQA	MANIQA	DOVER	# Params (M)
A				✓		✓	0.5707	0.4360	61.93	0.7571	4.4/1804
B	✓			✓		✓	0.5759	0.4467	63.86	0.7564	4.4/1906
C	✓	✓		✓		✓	0.5792	0.4547	63.93	0.7676	7.3/1909
D	✓	✓	✓	✓		✓	0.5824	<u>0.4572</u>	<u>64.25</u>	<u>0.7704</u>	10.5/1912
E	✓	✓	✓		✓		0.5851	0.4524	64.09	0.7665	10.5/1912
Ours	✓	✓	✓		✓	✓	0.5907	0.4599	64.42	0.7785	10.5/1912

**Figure 7: Temporal consistency analysis across SISR, VSR approaches, and different model variants.**

long inference times, especially for 2K video, making them impractical for real-world deployment. Thanks to the efficient one-step diffusion space, our UltraVSR significantly reduces inference time, taking only **0.06×** and **0.08×** that of the second fastest approach at two resolutions. Moreover, UltraVSR has substantially fewer trainable parameters (just **10.5M**) compared to other diffusion-based methods, underscoring its efficiency during the training process.

4.3 Ablation Study

We conduct comprehensive experiments to evaluate the contributions of the key components in UltraVSR. The results are presented in Tab. 3 and Fig. 7. We begin with Model A, which serves as our baseline, constructed by: (1) fixing the diffusion time step to 999, following the one-step generation paradigm established in prior works [10, 31, 52, 59]; (2) enabling only the trainable LoRA layers; and (3) replacing our proposed Spatio-temporal Joint Distillation (SJD) with the conventional Variational Score Distillation (VSD) [46, 59]. Due to its inability to dynamically perceive degradation levels, Model A exhibits limited reconstruction quality compared to Model B (with DRS). We incrementally enhance Model B with trainable RTS-convolution and RTS-attention units to form Models C and D, respectively, leading to steadily improved inter-frame consistency. We further evaluate the effectiveness of SJD and TAI by comparing Model D, Model E (with a fixed local sequence

of length 10), and our model. It can be seen that SJD significantly enhances temporal coherence by introducing inter-frame difference supervision, leading to improved motion continuity across frames compared to VSD [46, 59]. TAI further boosts performance by enabling long-range temporal modeling.

5 Conclusion

We present UltraVSR, the first real-world VSR framework based on an efficient one-step diffusion space. It introduces Degradation-aware Reconstruction Scheduling (DRS) to transform multi-step denoising with one-step LR-to-HR reconstruction. To maintain temporal consistency, we develop the Recurrent Temporal Shift (RTS) module and Spatio-temporal Joint Distillation (SJD) for realistic and coherent outputs, along with Temporally Asynchronous Inference (TAI) for efficient long-range temporal modeling. Extensive experiments show that UltraVSR delivers favorable performance with significantly accelerated inference speed.

6 Acknowledgments

This work was supported in part by the National Major Science and Technology Projects of China under Grant 2009XJTU0016, in part by the National Natural Science Foundation of China under Grant U22B2049.

References

- [1] Zekun Ai, Xiaotong Luo, Yanyun Qu, and Yuan Xie. 2024. SkipVSR: Adaptive Patch Routing for Video Super-Resolution with Inter-Frame Mask. In *Proceedings of the 32nd ACM International Conference on Multimedia*. 5874–5882.
- [2] Yuval Alaluf, Daniel Garibi, Or Patashnik, Hadar Averbuch-Elor, and Daniel Cohen-Or. 2024. Cross-image attention for zero-shot appearance transfer. In *ACM SIGGRAPH 2024 Conference Papers*. 1–12.
- [3] Andreas Blattmann, Robin Rombach, Huan Ling, Tim Dockhorn, Seung Wook Kim, Sanja Fidler, and Karsten Kreis. 2023. Align your latents: High-resolution video synthesis with latent diffusion models. In *Proceedings of the IEEE/CVF Conference on Computer Vision and Pattern Recognition*. 22563–22575.
- [4] Yochai Blau and Tomer Michaeli. 2018. The perception-distortion tradeoff. In *Proceedings of the IEEE conference on computer vision and pattern recognition*. 6228–6237.
- [5] Mingdeng Cao, Xintao Wang, Zhongang Qi, Ying Shan, Xiaohu Qie, and Yinqiang Zheng. 2023. Masactrl: Tuning-free mutual self-attention control for consistent image synthesis and editing. In *Proceedings of the IEEE/CVF international conference on computer vision*. 22560–22570.
- [6] Kelvin CK Chan, Xintao Wang, Ke Yu, Chao Dong, and Chen Change Loy. 2021. Basicvsr: The search for essential components in video super-resolution and beyond. In *Proceedings of the IEEE/CVF conference on computer vision and pattern recognition*. 4947–4956.
- [7] Kelvin CK Chan, Shangchen Zhou, Xiangyu Xu, and Chen Change Loy. 2022. Basicvsr++: Improving video super-resolution with enhanced propagation and alignment. In *Proceedings of the IEEE/CVF conference on computer vision and pattern recognition*. 5972–5981.
- [8] Kelvin CK Chan, Shangchen Zhou, Xiangyu Xu, and Chen Change Loy. 2022. Investigating tradeoffs in real-world video super-resolution. In *Proceedings of the IEEE/CVF Conference on Computer Vision and Pattern Recognition*. 5962–5971.
- [9] Prafulla Dhariwal and Alexander Nichol. 2021. Diffusion models beat gans on image synthesis. *Advances in neural information processing systems* 34 (2021), 8780–8794.
- [10] Kevin Frans, Danijar Hafner, Sergey Levine, and Pieter Abbeel. 2024. One step diffusion via shortcut models. *arXiv preprint arXiv:2410.12557* (2024).
- [11] Dario Fuoli, Shuhang Gu, and Radu Timofte. 2019. Efficient video super-resolution through recurrent latent space propagation. In *2019 IEEE/CVF International Conference on Computer Vision Workshop (ICCVW)*. IEEE, 3476–3485.
- [12] Michal Geyer, Omer Bar-Tal, Shai Bagon, and Tali Dekel. 2023. Tokenflow: Consistent diffusion features for consistent video editing. *arXiv preprint arXiv:2307.10373* (2023).
- [13] Jinjin Gu, Haoming Cai, Chao Dong, Jimmy S Ren, Radu Timofte, Yuan Gong, Shanshan Lao, Shuwei Shi, Jiahao Wang, Sidi Yang, et al. 2022. NTIRE 2022 challenge on perceptual image quality assessment. In *Proceedings of the IEEE/CVF conference on computer vision and pattern recognition*. 951–967.
- [14] Akash Gupta, Padmaja Jonnalagedda, Bir Bhanu, and Amit K Roy-Chowdhury. 2021. Ada-vsr: Adaptive video super-resolution with meta-learning. In *Proceedings of the 29th ACM international conference on multimedia*. 327–336.
- [15] Jonathan Ho, Ajay Jain, and Pieter Abbeel. 2020. Denoising diffusion probabilistic models. *Advances in neural information processing systems* 33 (2020), 6840–6851.
- [16] Edward J Hu, Yelong Shen, Phillip Wallis, Zeyuan Allen-Zhu, Yuanzhi Li, Shean Wang, Lu Wang, Weizhu Chen, et al. 2022. Lora: Low-rank adaptation of large language models. *ICLR* 1, 2 (2022), 3.
- [17] Shuo Jin, Meiqin Liu, Chao Yao, Chunyu Lin, and Yao Zhao. 2023. Kernel dimension matters: To activate available kernels for real-time video super-resolution. In *Proceedings of the 31st ACM International Conference on Multimedia*. 8617–8625.
- [18] Gu Jinjin, Cai Haoming, Chen Haoyu, Ye Xiaoxing, Jimmy S Ren, and Dong Chao. 2020. Pipal: a large-scale image quality assessment dataset for perceptual image restoration. In *Computer Vision—ECCV 2020: 16th European Conference, Glasgow, UK, August 23–28, 2020, Proceedings, Part XI* 16. Springer, 633–651.
- [19] Bahjat Kawar, Shiran Zada, Oran Lang, Omer Tov, Huiwen Chang, Tali Dekel, Inbar Mosseri, and Michal Irani. 2023. Imagic: Text-based real image editing with diffusion models. In *Proceedings of the IEEE/CVF conference on computer vision and pattern recognition*. 6007–6017.
- [20] Junjie Ke, Qifei Wang, Yilin Wang, Peyman Milanfar, and Feng Yang. 2021. Musiq: Multi-scale image quality transformer. In *Proceedings of the IEEE/CVF international conference on computer vision*. 5148–5157.
- [21] Diederik P Kingma and Jimmy Ba. 2014. Adam: A method for stochastic optimization. *arXiv preprint arXiv:1412.6980* (2014).
- [22] Christian Ledig, Lucas Theis, Ferenc Huszar, Jose Caballero, Andrew Cunningham, Alejandro Acosta, Andrew Aitken, Alykhan Tejani, Johannes Totz, Zehan Wang, et al. 2017. Photo-realistic single image super-resolution using a generative adversarial network. In *Proceedings of the IEEE conference on computer vision and pattern recognition*. 4681–4690.
- [23] Jiayu Leng, Jia Wang, Xinbo Gao, Bo Hu, Ji Gan, and Chenqiang Gao. 2022. Icnct: Joint alignment and reconstruction via iterative collaboration for video super-resolution. In *Proceedings of the 30th ACM International Conference on Multimedia*. 6675–6684.
- [24] Dasong Li, Xiaoyu Shi, Yi Zhang, Ka Chun Cheung, Simon See, Xiaogang Wang, Hongwei Qin, and Hongsheng Li. 2023. A simple baseline for video restoration with grouped spatial-temporal shift. In *Proceedings of the IEEE/CVF Conference on Computer Vision and Pattern Recognition*. 9822–9832.
- [25] Yinchuan Li, Xinyu Shao, Jianping Zhang, Haozhi Wang, Leo Maxime Brunswic, Kaiwen Zhou, Jiqian Dong, Kaiyang Guo, Xiu Li, Zhitang Chen, et al. 2025. Generative models in decision making: A survey. *arXiv preprint arXiv:2502.17100* (2025).
- [26] Jingyu Liang, Jiezhong Cao, Yuchen Fan, Kai Zhang, Rakesh Ranjan, Yawei Li, Radu Timofte, and Luc Van Gool. 2024. Vrt: A video restoration transformer. *IEEE Transactions on Image Processing* (2024).
- [27] Jingyun Liang, Yuchen Fan, Xiaoyu Xiang, Rakesh Ranjan, Eddy Ilg, Simon Green, Jiezhong Cao, Kai Zhang, Radu Timofte, and Luc V Gool. 2022. Recurrent video restoration transformer with guided deformable attention. *Advances in Neural Information Processing Systems* 35 (2022), 378–393.
- [28] Ji Lin, Chuang Gan, and Song Han. 2019. Tsm: Temporal shift module for efficient video understanding. In *Proceedings of the IEEE/CVF international conference on computer vision*. 7083–7093.
- [29] Andres Munoz, Mohammadreza Zolfaghari, Max Argus, and Thomas Brox. 2021. Temporal shift GAN for large scale video generation. In *Proceedings of the IEEE/CVF Winter Conference on Applications of Computer Vision*. 3179–3188.
- [30] Seungjun Nah, Sungyong Baik, Seokil Hong, Gyeongsik Moon, Sanghyun Son, Radu Timofte, and Kyoung Mu Lee. 2019. Ntire 2019 challenge on video deblurring and super-resolution: Dataset and study. In *Proceedings of the IEEE/CVF conference on computer vision and pattern recognition workshops*. 0–0.
- [31] Thuan Hoang Nguyen and Anh Tran. 2024. Swiftbrush: One-step text-to-image diffusion model with variational score distillation. In *Proceedings of the IEEE/CVF Conference on Computer Vision and Pattern Recognition*. 7807–7816.
- [32] Anton Lozhkov Pedro Cuenca Nathan Lambert Kashif Rasul Mishig Davaadorj Patrick von Platen, Suraj Patil and Thomas Wolf. 2022. Diffusers: State-of-the-art Diffusion Models.
- [33] Ben Poole, Ajay Jain, Jonathan T Barron, and Ben Mildenhall. 2022. Dreamfusion: Text-to-3d using 2d diffusion. *arXiv preprint arXiv:2209.14988* (2022).
- [34] Robin Rombach, Andreas Blattmann, Dominik Lorenz, Patrick Esser, and Björn Ommer. 2022. High-resolution image synthesis with latent diffusion models. In *Proceedings of the IEEE/CVF conference on computer vision and pattern recognition*. 10684–10695.
- [35] Xiaoyu Shi, Zhaoyang Huang, Fu-Yun Wang, Weikang Bian, Dasong Li, Yi Zhang, Manyuan Zhang, Ka Chun Cheung, Simon See, Hongwei Qin, et al. 2024. Motion-i2v: Consistent and controllable image-to-video generation with explicit motion modeling. In *ACM SIGGRAPH 2024 Conference Papers*. 1–11.
- [36] Jascha Sohl-Dickstein, Eric Weiss, Niru Maheswaranathan, and Surya Ganguli. 2015. Deep unsupervised learning using nonequilibrium thermodynamics. In *International conference on machine learning*. PMLR, 2256–2265.
- [37] Yang Song, Prafulla Dhariwal, Mark Chen, and Ilya Sutskever. 2023. Consistency models. (2023).
- [38] Luming Tang, Menglin Jia, Qianqian Wang, Cheng Perng Phoo, and Bharath Hariharan. 2023. Emergent correspondence from image diffusion. *Advances in Neural Information Processing Systems* 36 (2023), 1363–1389.
- [39] Xin Tao, Hongyun Gao, Renjie Liao, Jue Wang, and Jiaya Jia. 2017. Detail-revealing deep video super-resolution. In *Proceedings of the IEEE international conference on computer vision*. 4472–4480.
- [40] Pascal Vincent. 2011. A connection between score matching and denoising autoencoders. *Neural computation* 23, 7 (2011), 1661–1674.
- [41] Jianyi Wang, Kelvin CK Chan, and Chen Change Loy. 2023. Exploring clip for assessing the look and feel of images. In *Proceedings of the AAAI conference on artificial intelligence*, Vol. 37. 2555–2563.
- [42] Jiangang Wang, Qingnan Fan, Qi Zhang, Haigen Liu, Yuhang Yu, Jinwei Chen, and Wenqi Ren. 2024. Hero-SR: One-Step Diffusion for Super-Resolution with Human Perception Priors. *arXiv preprint arXiv:2412.07152* (2024).
- [43] Jianyi Wang, Zongsheng Yue, Shangchen Zhou, Kelvin CK Chan, and Chen Change Loy. 2024. Exploiting diffusion prior for real-world image super-resolution. *International Journal of Computer Vision* (2024), 1–21.
- [44] Xintao Wang, Liangbin Xie, Chao Dong, and Ying Shan. 2021. Real-esrgan: Training real-world blind super-resolution with pure synthetic data. In *Proceedings of the IEEE/CVF international conference on computer vision*. 1905–1914.
- [45] Yufei Wang, Wenhan Yang, Xinyuan Chen, Yaohui Wang, Lanqing Guo, Lap-Pui Chau, Ziwei Liu, Yu Qiao, Alex C Kot, and Bihan Wen. 2024. Sinsr: diffusion-based image super-resolution in a single step. In *Proceedings of the IEEE/CVF conference on computer vision and pattern recognition*. 25796–25805.
- [46] Zhengyi Wang, Cheng Lu, Yikai Wang, Fan Bao, Chongxuan Li, Hang Su, and Jun Zhu. 2023. Prolificdreamer: High-fidelity and diverse text-to-3d generation with variational score distillation. *Advances in Neural Information Processing Systems* 36 (2023), 8406–8441.
- [47] Haoning Wu, Erli Zhang, Liang Liao, Chaofeng Chen, Jingwen Hou, Annan Wang, Wenxiu Sun, Qiong Yan, and Weisi Lin. 2023. Exploring video quality assessment on user generated contents from aesthetic and technical perspectives.

- In *Proceedings of the IEEE/CVF International Conference on Computer Vision*. 20144–20154.
- [48] Rongyuan Wu, Lingchen Sun, Zhiyuan Ma, and Lei Zhang. 2024. One-step effective diffusion network for real-world image super-resolution. *Advances in Neural Information Processing Systems* 37 (2024), 92529–92553.
- [49] Zeyu Xiao, Dachun Kai, Yueyi Zhang, Xiaoyan Sun, and Zhiwei Xiong. 2024. Asymmetric Event-Guided Video Super-Resolution. In *Proceedings of the 32nd ACM International Conference on Multimedia*. 2409–2418.
- [50] Zeyu Xiao, Zhiwei Xiong, Xueyang Fu, Dong Liu, and Zheng-Jun Zha. 2020. Space-time video super-resolution using temporal profiles. In *Proceedings of the 28th ACM International Conference on Multimedia*. 664–672.
- [51] Rui Xie, Yinhong Liu, Penghao Zhou, Chen Zhao, Jun Zhou, Kai Zhang, Zhenyu Zhang, Jian Yang, Zhenheng Yang, and Ying Tai. 2025. STAR: Spatial-Temporal Augmentation with Text-to-Video Models for Real-World Video Super-Resolution. *arXiv preprint arXiv:2501.02976* (2025).
- [52] Rui Xie, Chen Zhao, Kai Zhang, Zhenyu Zhang, Jun Zhou, Jian Yang, and Ying Tai. 2024. Addsr: Accelerating diffusion-based blind super-resolution with adversarial diffusion distillation. *arXiv preprint arXiv:2404.01717* (2024).
- [53] Binxin Yang, Shuyang Gu, Bo Zhang, Ting Zhang, Xuejin Chen, Xiaoyan Sun, Dong Chen, and Fang Wen. 2023. Paint by example: Exemplar-based image editing with diffusion models. In *Proceedings of the IEEE/CVF Conference on Computer Vision and Pattern Recognition*. 18381–18391.
- [54] Sidi Yang, Tianhe Wu, Shuwei Shi, Shanshan Lao, Yuan Gong, Mingdeng Cao, Jiahao Wang, and Yujiu Yang. 2022. Maniqa: Multi-dimension attention network for no-reference image quality assessment. In *Proceedings of the IEEE/CVF conference on computer vision and pattern recognition*. 1191–1200.
- [55] Xi Yang, Chenhang He, Jianqi Ma, and Lei Zhang. 2025. Motion-guided latent diffusion for temporally consistent real-world video super-resolution. In *European Conference on Computer Vision*. Springer, 224–242.
- [56] Zhuoyi Yang, Jiayan Teng, Wendi Zheng, Ming Ding, Shiyu Huang, Jiazheng Xu, Yuanming Yang, Wenyi Hong, Xiaohan Zhang, Guanyu Feng, et al. 2024. Cogvideox: Text-to-video diffusion models with an expert transformer. *arXiv preprint arXiv:2408.06072* (2024).
- [57] Peng Yi, Zhongyuan Wang, Kui Jiang, Junjun Jiang, Tao Lu, Xin Tian, and Jiayi Ma. 2021. Omniscient video super-resolution. In *Proceedings of the IEEE/CVF international conference on computer vision*. 4429–4438.
- [58] Peng Yi, Zhongyuan Wang, Kui Jiang, Junjun Jiang, and Jiayi Ma. 2019. Progressive fusion video super-resolution network via exploiting non-local spatio-temporal correlations. In *Proceedings of the IEEE/CVF international conference on computer vision*. 3106–3115.
- [59] Tianwei Yin, Michaël Gharbi, Richard Zhang, Eli Shechtman, Fredo Durand, William T Freeman, and Taesung Park. 2024. One-step diffusion with distribution matching distillation. In *Proceedings of the IEEE/CVF conference on computer vision and pattern recognition*. 6613–6623.
- [60] Fanghua Yu, Jinjin Gu, Zheyuan Li, Jinfan Hu, Xiangtao Kong, Xintao Wang, Jingwen He, Yu Qiao, and Chao Dong. 2024. Scaling up to excellence: Practicing model scaling for photo-realistic image restoration in the wild. In *Proceedings of the IEEE/CVF Conference on Computer Vision and Pattern Recognition*. 25669–25680.
- [61] Zongsheng Yue, Jianyi Wang, and Chen Change Loy. 2024. Resshift: Efficient diffusion model for image super-resolution by residual shifting. *Advances in Neural Information Processing Systems* 36 (2024).
- [62] Lvmin Zhang, Anyi Rao, and Maneesh Agrawala. 2023. Adding conditional control to text-to-image diffusion models. In *Proceedings of the IEEE/CVF International Conference on Computer Vision*. 3836–3847.
- [63] Yuehan Zhang and Angela Yao. 2024. Realviformer: Investigating attention for real-world video super-resolution. In *European Conference on Computer Vision*. Springer, 412–428.
- [64] Shangchen Zhou, Chongyi Li, Kelvin CK Chan, and Chen Change Loy. 2023. Propainter: Improving propagation and transformer for video inpainting. In *Proceedings of the IEEE/CVF international conference on computer vision*. 10477–10486.
- [65] Shangchen Zhou, Peiqing Yang, Jianyi Wang, Yihang Luo, and Chen Change Loy. 2024. Upscale-A-Video: Temporal-Consistent Diffusion Model for Real-World Video Super-Resolution. In *Proceedings of the IEEE/CVF Conference on Computer Vision and Pattern Recognition*. 2535–2545.

Supplementary Material for "UltraVSR: Achieving Ultra-Realistic Video Super-Resolution with Efficient One-Step Diffusion Space"

Yong Liu
Xi'an Jiaotong University
Xi'an, China
liuy1996v@qq.com

Jinshan Pan
Nanjing University of Science and
Technology
Nanjing, China
sdluran@gmail.com

Yinchuan Li
Huawei Noah's Ark Lab
Beijing, China

Qingji Dong
Xi'an Jiaotong University
Xi'an, China

Chao Zhu
Xi'an Jiaotong University
Xi'an, China

Yu Guo
Xi'an Jiaotong University
Xi'an, China

Fei Wang*
Xi'an Jiaotong University
Xi'an, China
wfx@xjtu.edu.cn

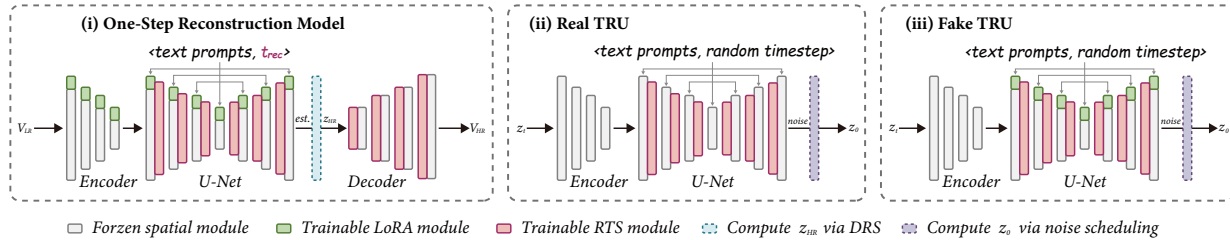


Figure 1: The detailed network structure of different models in the proposed UltraVSR.

CCS Concepts

• **Computing methodologies** → **Reconstruction**; *Image processing*; Computational photography.

Keywords

Video super-resolution, Diffusion model, Temporal consistency

ACM Reference Format:

Yong Liu, Jinshan Pan, Yinchuan Li, Qingji Dong, Chao Zhu, Yu Guo, and Fei Wang. 2025. Supplementary Material for "UltraVSR: Achieving Ultra-Realistic Video Super-Resolution with Efficient One-Step Diffusion Space". In *Proceedings of the 33rd ACM International Conference on Multimedia (MM '25)*, October 27–31, 2025, Dublin, Ireland. ACM, New York, NY, USA, 4 pages. <https://doi.org/10.1145/3746027.3755117>

*Corresponding author. Author affiliation: National Key Laboratory of Human-Machine Hybrid Augmented Intelligence, National Engineering Research Center of Visual Information and Applications, Institute of Artificial Intelligence and Robotics, Xi'an Jiaotong University.

Permission to make digital or hard copies of all or part of this work for personal or classroom use is granted without fee provided that copies are not made or distributed for profit or commercial advantage and that copies bear this notice and the full citation on the first page. Copyrights for components of this work owned by others than the author(s) must be honored. Abstracting with credit is permitted. To copy otherwise, or republish, to post on servers or to redistribute to lists, requires prior specific permission and/or a fee. Request permissions from permissions@acm.org.
MM '25, Dublin, Ireland.

© 2025 Copyright held by the owner/author(s). Publication rights licensed to ACM.
ACM ISBN 979-8-4007-2035-2/2025/10
<https://doi.org/10.1145/3746027.3755117>

1 Network Details

To address the challenges of real-world VSR, we present UltraVSR, an efficient one-step diffusion-based framework. UltraVSR comprises three core components: a one-step reconstruction model, a Real Temporal Regularized UNet (Real TRU), and a Fake Temporal Regularized UNet (Fake TRU). Their network structures are illustrated in Fig. 1.

1.1 One-step Reconstruction Model

By introducing a Degradation-aware Reconstruction Scheduling (DRS), our one-step reconstruction model enables direct one-step restoration from LR to HR videos. To adapt the pretrained generative prior to this paradigm, we integrate LoRA layers [2] into both the VAE encoder and the diffusion UNet. Moreover, since the inconsistency details in Stable Diffusion primarily stem from the diffusion UNet and VAE decoder [5, 6], we develop a lightweight yet effective Recurrent Temporal Shift (RTS) module to capture temporal consistency across frames and insert it into each scale of both the diffusion UNet and VAE decoder.

1.2 Real TRU and Fake TRU

To guide the one-step reconstruction model toward generating visually realistic and temporally consistent videos, we propose Spatio-temporal Joint Distillation (SJD), comprising a Real TRU and a Fake TRU. Both TRUs are adapted from the pretrained Stable

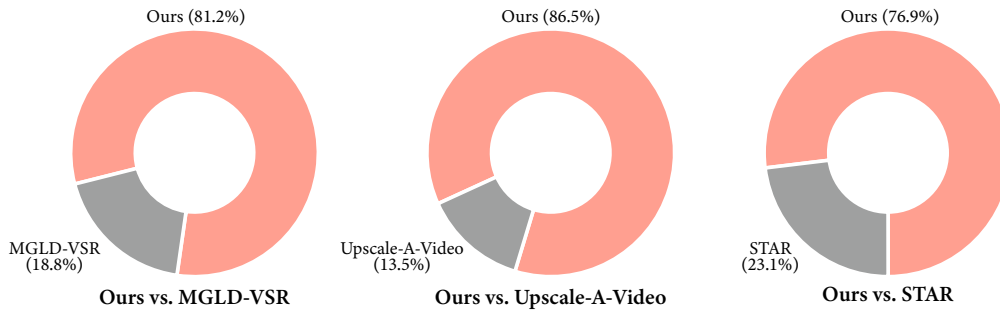


Figure 2: User study results. Our UltraVSR is consistently preferred by human evaluators over other methods.

Diffusion model [3] and updated to learn real/fake video distribution based on the samples from ground truth and reconstructed videos, respectively. To enable temporal modeling, we insert the proposed RTS modules into the diffusion UNet of both TRUs. In addition, the Fake TRU is equipped with LoRA layers to enhance its capacity for learning the synthesized video distribution.

2 Model Analysis

2.1 Unique design of RTS

Unlike previous works, our Recurrent Temporal Shift (RTS) module is specifically designed with the following unique features: (1) Dual-level temporal modeling: Following the standard architecture of diffusion models (i.e., convolution + attention), RTS integrates a RTS-Convolution Unit for local temporal continuity through convolution layers and a RTS-Attention Unit for global semantic alignment using the Mutual Self-Attention. (2) High efficiency: RTS is lightweight, with channel-reducing/increasing layers to minimize overhead, making it practical within diffusion-based pipelines.

2.2 Computational efficiency of TAI

Here, we analyze it from two perspectives: (1) TAI under memory-limited vs. non-TAI under larger-memory conditions: While larger memory enables faster inference, our TAI is specifically designed for memory-limited conditions (e.g., 48GB). Without TAI, prior methods must split videos into short clips, which disrupts temporal continuity. In contrast, TAI allows processing up to 120 frames at 2K resolution. (2) TAI vs. non-TAI under memory-limited conditions: In Tab. 2, we compare our method (with TAI) with MGLD-VSR (without TAI), both using the same backbone. Our method is 35.7× faster at 720p and 76.4× faster at 2K resolution, benefiting not only from fewer sampling steps but also from the efficient TAI module.

2.3 Difference between Real TRU and fake TRU

The Real TRU and Fake TRU differ in both structure and training strategy. Structurally, both variants consist of a frozen SD model and trainable RTS modules; however, Fake TRU additionally includes a trainable LoRA module. During the training of the One-Step VSR model, all other components are frozen, and both Real TRU and Fake TRU take the reconstructed HR video as input for computing the SJD loss. When updating Real TRU specifically, its input is the ground-truth video, and the loss follows the standard denoising objective [3]. In contrast, Fake TRU is updated using the reconstructed HR video as input, also supervised by the standard denoising objective [3].

3 User Study

To strengthen claims of visual realism of our method, we conducted a user study to assess the perceptual quality of real-world videos generated by various diffusion-based VSR methods, including Upscale-A-Video [6], MGLD-VSR [5], STAR [4], and our proposed method. We recruited 20 participants, each of whom viewed 20 randomly selected video triplets. Each triplet consisted of the input low-resolution video, the output of one competing method, and the output of our method. The order of the compared outputs was randomized. Participants were asked to select the video that appeared visually more realistic and temporally consistent. The results are shown in Fig. 2. Our approach gains more votes in the competitions.

4 More Visual Results

As shown in Fig. 3 and Fig. 4, we present more visual comparisons and temporal consistency analysis with the state-of-the-art approaches. These results demonstrate that UltraVSR not only excels in perceptual quality but also maintains strong temporal coherence.

5 Video Demo

We provide a **video demo** to showcase more video comparison results with both diffusion-based SISR and VSR approaches.

References

- [1] Kelvin CK Chan, Shangchen Zhou, Xiangyu Xu, and Chen Change Loy. 2022. Investigating tradeoffs in real-world video super-resolution. In *Proceedings of the IEEE/CVF Conference on Computer Vision and Pattern Recognition*. 5962–5971.
- [2] Edward J Hu, Yelong Shen, Phillip Wallis, Zeyuan Allen-Zhu, Yuanzhi Li, Shean Wang, Lu Wang, Weizhu Chen, et al. 2022. Lora: Low-rank adaptation of large language models. *ICLR* 1, 2 (2022), 3.
- [3] Robin Rombach, Andreas Blattmann, Dominik Lorenz, Patrick Esser, and Björn Ommer. 2022. High-resolution image synthesis with latent diffusion models. In *Proceedings of the IEEE/CVF conference on computer vision and pattern recognition*. 10684–10695.
- [4] Rui Xie, Yinhong Liu, Penghao Zhou, Chen Zhao, Jun Zhou, Kai Zhang, Zhenyu Zhang, Jian Yang, Zhenheng Yang, and Ying Tai. 2025. STAR: Spatial-Temporal Augmentation with Text-to-Video Models for Real-World Video Super-Resolution. *arXiv preprint arXiv:2501.02976* (2025).
- [5] Xi Yang, Chenhang He, Jianqi Ma, and Lei Zhang. 2025. Motion-guided latent diffusion for temporally consistent real-world video super-resolution. In *European Conference on Computer Vision*. Springer, 224–242.
- [6] Shangchen Zhou, Peiqing Yang, Jianyi Wang, Yihang Luo, and Chen Change Loy. 2024. Upscale-A-Video: Temporal-Consistent Diffusion Model for Real-World Video Super-Resolution. In *Proceedings of the IEEE/CVF Conference on Computer Vision and Pattern Recognition*. 2535–2545.

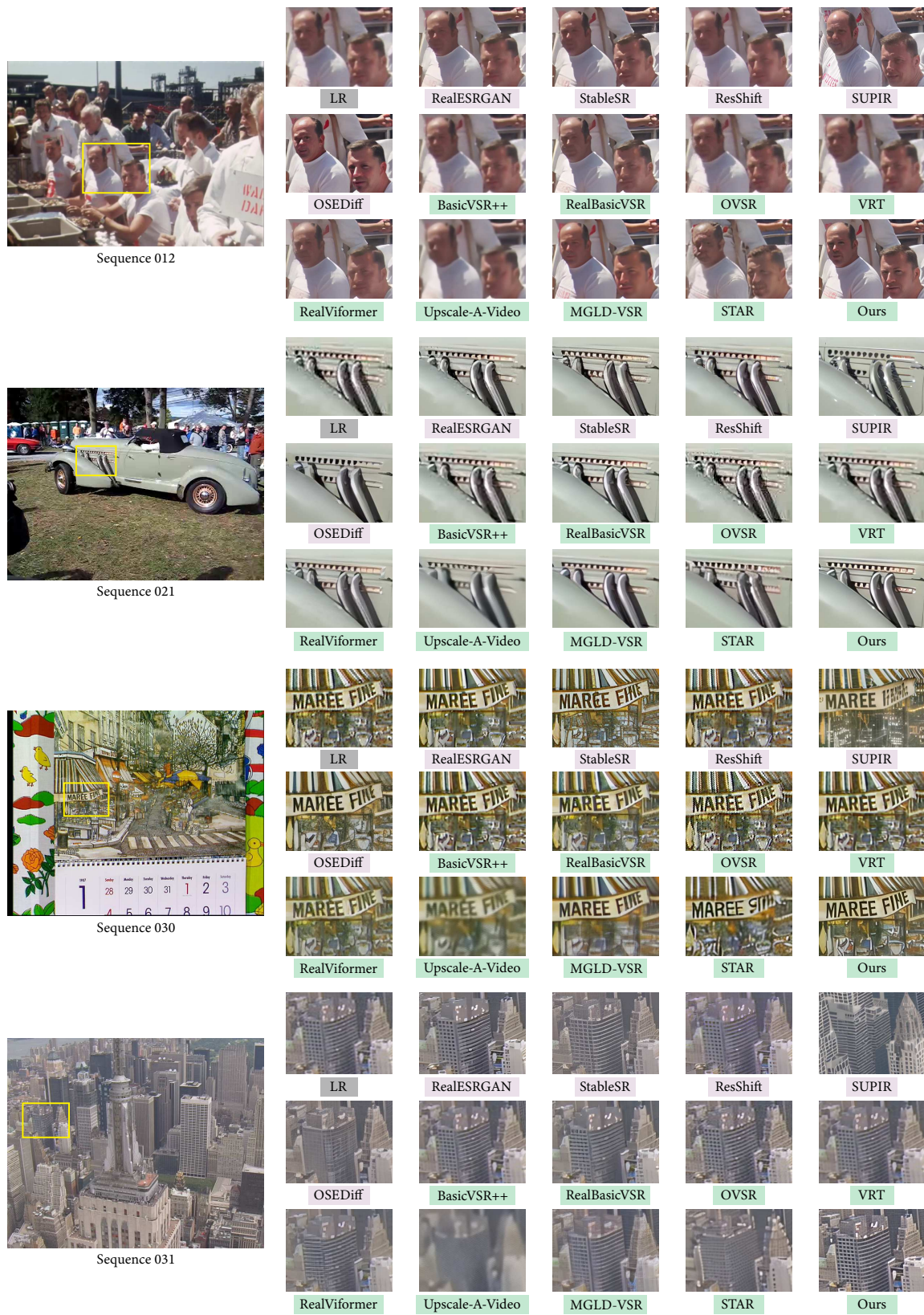


Figure 3: More visual comparisons both **SISR** and **VSR** methods on real-world low-quality videos from VideoLQ [1] dataset.



Figure 4: Temporal consistency analysis across both SISR and VSR methods.